FORENSIC EVIDENCE SUMMARY

Analysis of Physical Evidence and Video Forensics

Incident at Utah Valley University (UVU)

September 10, 2024

PREPARED FOR THE DEFENSE TEAM

CONFIDENTIAL — ATTORNEY WORK PRODUCT

Compiled by: Jon Aaron Bray

Forensic Video Analysis and Technical Research

Date of Report: February 9, 2026

Table of Contents

1. Executive Summary

This report presents forensic evidence gathered from multiple eyewitness video recordings and physical evidence related to the incident that occurred on September 10, 2024, at Utah Valley University (UVU). The evidence presented herein has been compiled to support the defense of the accused individual and demonstrates that the injuries sustained by the victim may have originated from the catastrophic failure or energetic disruption of a RODE Wireless PRO transmitter microphone worn underneath the victim's shirt, rather than from the actions attributed to the accused.

The combined weight of the physical evidence, video analysis, pixel flow mapping, and temporal sequencing of events supports an alternative explanation for the injuries observed. This report is organized to present the evidence systematically, beginning with the physical components involved, followed by the video forensic analysis, and concluding with a synthesis of findings.

Key Finding: The epicenter of the physical disturbance documented on video corresponds precisely with the location of the RODE Wireless PRO transmitter worn under the victim's shirt. The sequence of events—including shirt deformation from expanding gases, shrapnel trajectories, necklace displacement, and the delayed onset of bleeding—is consistent with an energetic event originating from within or at the transmitter, not from an external projectile wound to the neck.

2. The RODE Wireless PRO Transmitter

Understanding the physical construction of the device worn by the victim is essential to interpreting the video evidence. The following images show an identical RODE Wireless PRO transmitter unit that has been disassembled to document its internal components. This is the same model worn by the victim on September 10, 2024.

2.1 Device Overview

The RODE Wireless PRO is a compact wireless microphone transmitter measuring approximately 44mm x 46mm x 18mm. It features a polycarbonate and glass front face with an OLED screen, and attaches to clothing via a magnetic clip system. The transmitter is designed to be worn clipped to the outside of clothing, or concealed underneath clothing with the magnetic clip holding it in place through the fabric.

Exhibit A-3: RODE Wireless PRO transmitter exterior. Note the glass front face (shown cracked in this exemplar unit). The device measures approximately 44mm x 46mm.

2.2 Internal Components

The disassembled transmitter reveals three primary internal components of forensic significance:

1. **Lithium Polymer (LiPo) Battery:** A rectangular lithium polymer cell (approximately 27.7mm x 23mm x 6.2mm) with a 3-wire JST connector. This battery stores significant energy and, if subjected to mechanical stress, puncture, or thermal runaway, is capable of rapid energy release including gas generation, fire, and explosive decompression.

2. **Printed Circuit Board (PCB):** A compact circuit board (approximately 30mm x 28mm) containing the ARM processor, radio transceiver, OLED driver, USB-C charging port, and other surface-mount components. The board is marked ‘RODE WIRELESS PRO (TX)’ with date codes visible. This rigid rectangular component is a key object tracked in the video analysis.
3. **Magnetic Clip Assembly:** A rectangular neodymium magnet approximately 25mm x 12mm used to secure the transmitter through clothing fabric. This component was observed following a trajectory consistent with the PCB and battery but lagging behind in velocity.

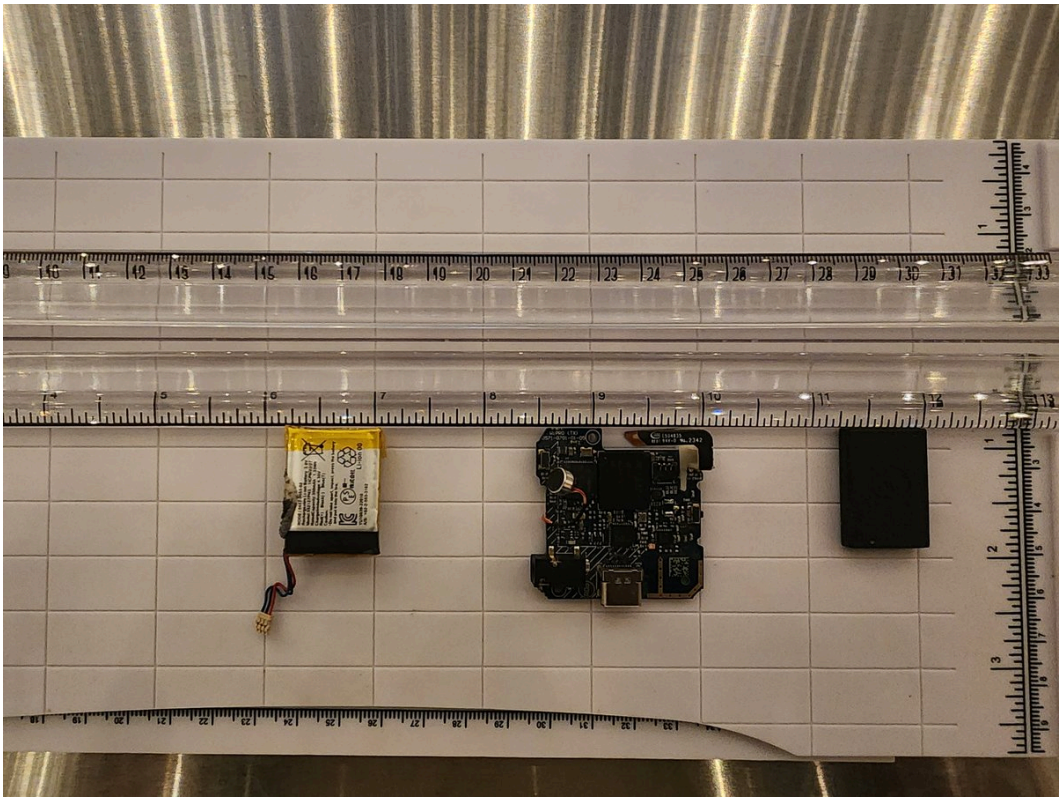

Exhibit A-1: RODE Wireless PRO transmitter disassembled (front view). Top: LiPo battery with JST connector. Middle: Main PCB with USB-C port, ARM processor, and radio components. Bottom: Magnetic clip assembly. Ruler scale in inches and centimeters.

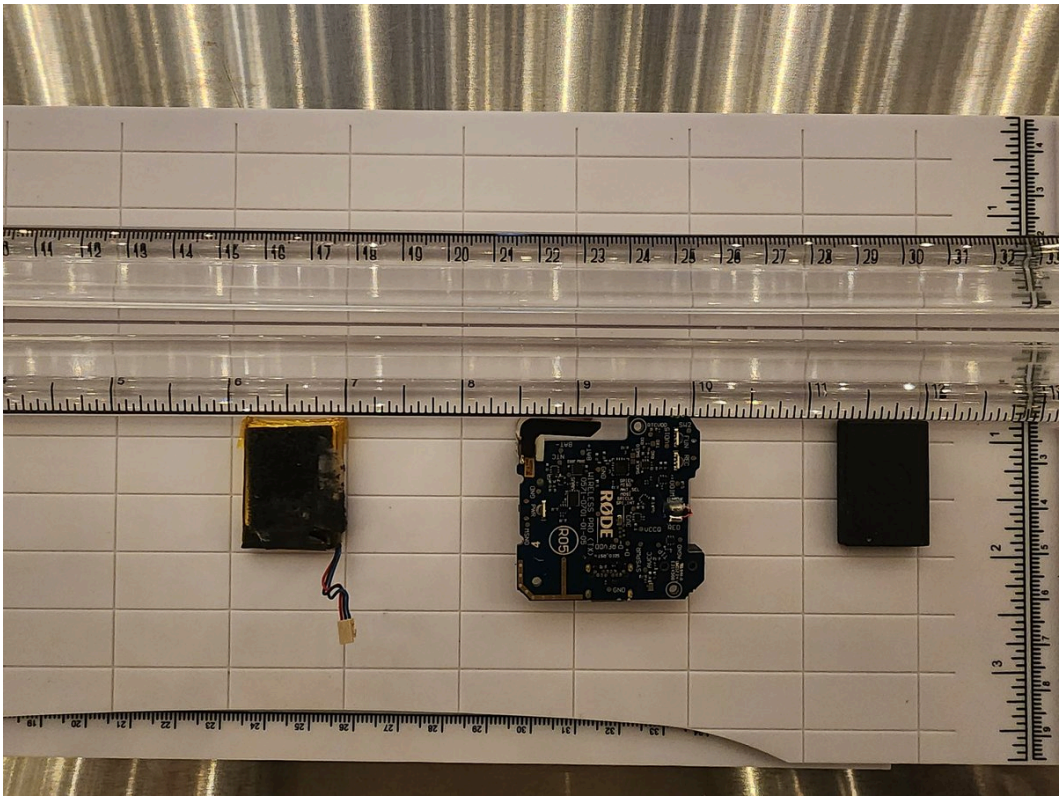

Exhibit A-2: RODE Wireless PRO transmitter disassembled (rear view). PCB reverse side clearly marked 'RODE WIRELESS PRO (TX)' with manufacturing date codes.

3. Physical Evidence from the Scene

3.1 Damaged Transmitter

Photographs of the RODE Wireless PRO transmitter recovered from the scene show significant damage consistent with a catastrophic energetic event. The glass front face is shattered with enough force to shatter into small fragments. These fragments can be seen scattered on the floorboard of the SUV used to transport the victim to the hospital.

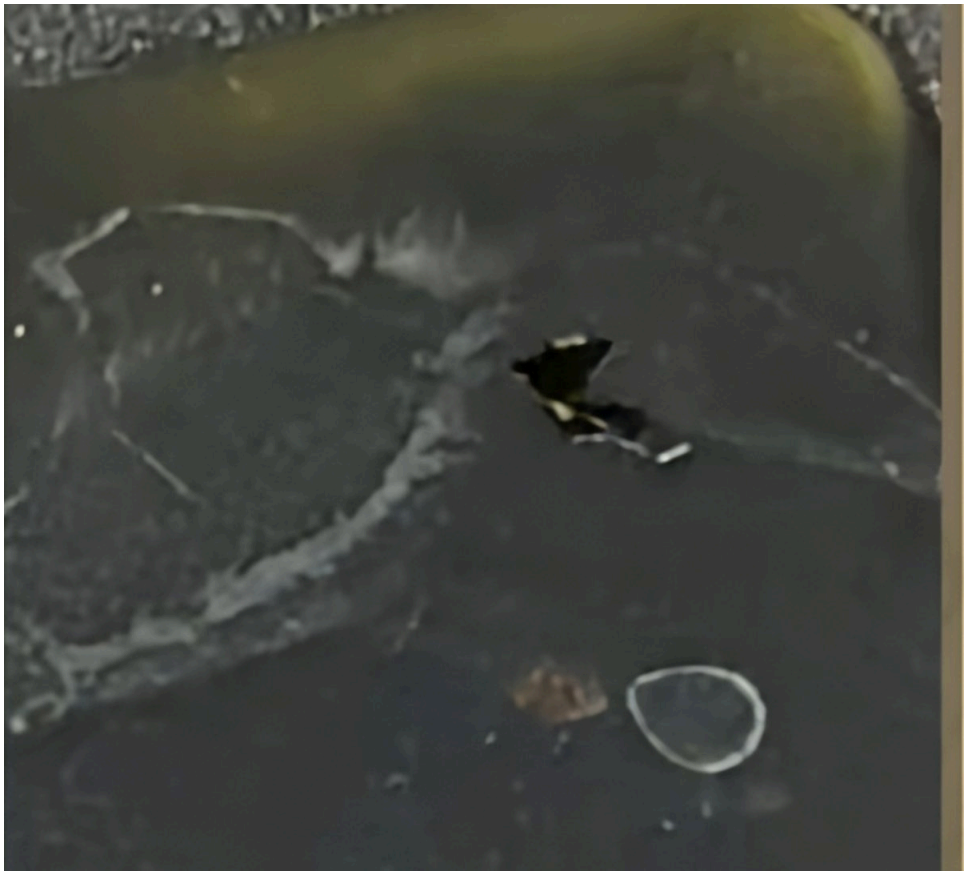

Exhibit C-1: Close-up of the damaged RODE Wireless PRO transmitter. Printed font and a beveled edge can be seen on the fragmentation. The beveled edge and printed font can be seen on the fragmentation.

Exhibit C-2: Composite image. Top left: Close-up of the damage to the transmitter glass face. Top right: Transmitter debris on the floorboard of the SUV that transported the victim to the hospital. Bottom: Intact RODE Wireless PRO transmitter for comparison.

3.2 Vehicle Floorboard Evidence

The SUV that transported the victim to the hospital contained fragmentation from the RODE Wireless PRO transmitter scattered across the floorboard beneath where the victim was placed. This debris field is consistent with the transmitter having been catastrophically disrupted, with glass fragments, circuit board pieces, and battery material separating from the device during or after the incident.

3.3 Scene Aftermath

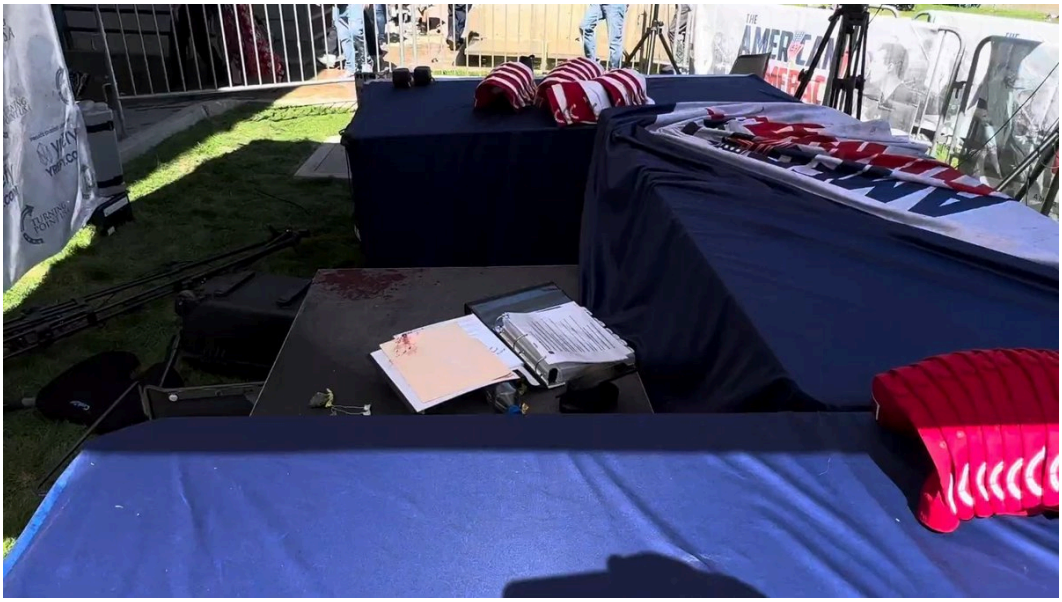

Exhibit B-2: Stage area aftermath. Blood spatter visible on documents and fragmentation on the table. Turning Point USA and YREFY branding visible, establishing the event context.

4. Video Forensic Analysis

Multiple eyewitness cell phone videos captured the incident from various angles. Frame-by-frame analysis of these recordings reveals a highly specific sequence of physical events that are inconsistent with a simple external projectile wound and instead point to the RODE Wireless PRO transmitter as the epicenter of an energetic disruption.

4.1 Multi-Camera Shutter Speed Evidence

A critical piece of evidence comes from comparing footage from two different cameras recording simultaneously at different frame rates. One iPhone recorded at 1080p/60fps while another recorded at 1080p/30fps. In the 30fps footage, the victim's shirt collar is fully stretched and expanded on the back right side. In the 60fps footage captured at the same moment, the collar is only partially stretched—still mid-deformation. This demonstrates that the shirt deformation occurred so rapidly that it fell between the shutter intervals of the two recordings, establishing that the expansive force was extremely fast-acting and violent.

Exhibit E-1: Side-by-side comparison from two simultaneous cameras (60fps left, 30fps right). The 30fps frame captures the collar fully stretched while the 60fps frame captures it mid-deformation, proving the extreme speed of the expansion event.

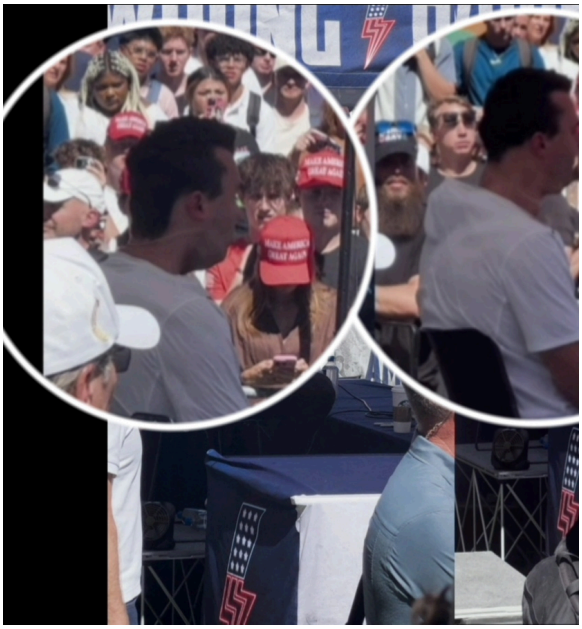

Exhibit E-2: Scene photograph with zoom insets showing bystander positions relative to the victim at the time of the incident.

4.2 Sequence of Events — Frame-by-Frame

The following sequence was reconstructed from multiple video angles at 30fps (approximately 33.3ms per frame). Times are relative to the first observable disturbance:

Phase 1: Pre-Deformation (T = 0ms)

Faint smoke or gas is visible escaping from the front of the victim's shirt collar in a single frame immediately preceding the dramatic physical events. This is consistent with a rapid gas-generating event (such as lithium battery thermal runaway or an energetic decomposition) occurring inside the shirt, beneath the transmitter location. The gas precedes mechanical displacement by one frame (~33ms), indicating the energy source generated expanding gases before the physical components were displaced.

Phase 2: Shirt Deformation and Component Displacement (T = 33–66ms)

The entire front of the victim's shirt experiences rapid deformation from expanding gases. The back of the shirt collar on the right side expands dramatically. The right sleeve deforms outward. These fabric movements are consistent with a sudden pressurization event underneath the shirt at the location of the transmitter (right side of chest, below the collarbone). Simultaneously, the victim's metal necklace is snapped by the force and sent flying upward and around his head, coming to rest on his left shoulder hanging from the shirt collar.

Exhibit D-2: Annotated frame showing the victim moments after the energetic event. Red arrows indicate the direction of shirt deformation and component displacement. The shirt collar is visibly distorted.

Phase 3: Circuit Board and Battery Trajectory (T = 33–99ms)

In a single frame of video, the circuit board from the RODE Wireless PRO transmitter is visible flying across the victim's shirt from right to left. The square shape of the PCB can be identified as it is briefly caught in the shirt collar over the victim's left cheek. The battery follows a similar trajectory, impacting the lower left portion of zone 2 of the victim's neck (left lateral neck). The circuit board nearly escapes the shirt collar entirely, leaving residue on the white shirt fabric. The magnetic clasp follows a similar trajectory but lags behind the PCB and battery, which moved at higher velocity due to their proximity to the energy source.

Exhibit F-1: Enhanced false-color heatmap visualization with the PCB component overlay at the detected location on the victim's neck/collar area, corresponding to where the PCB was caught in the shirt collar during its trajectory.

Phase 4: Battery Exit and Neck Wound (T = 443ms)

Approximately 0.443 seconds after the initial shirt deformation, the battery is observed falling out of the wound in the victim's neck. This is immediately followed by a heavy flow of blood from the rectangular wound. The wound shape is consistent with the rectangular profile of the LiPo battery (27.7mm x 23mm). The bleeding pattern—suppressed while the battery was lodged in the wound, then flowing heavily once the battery falls free—is consistent with removal of a tamponading foreign body from a venous wound affecting the external jugular vein.

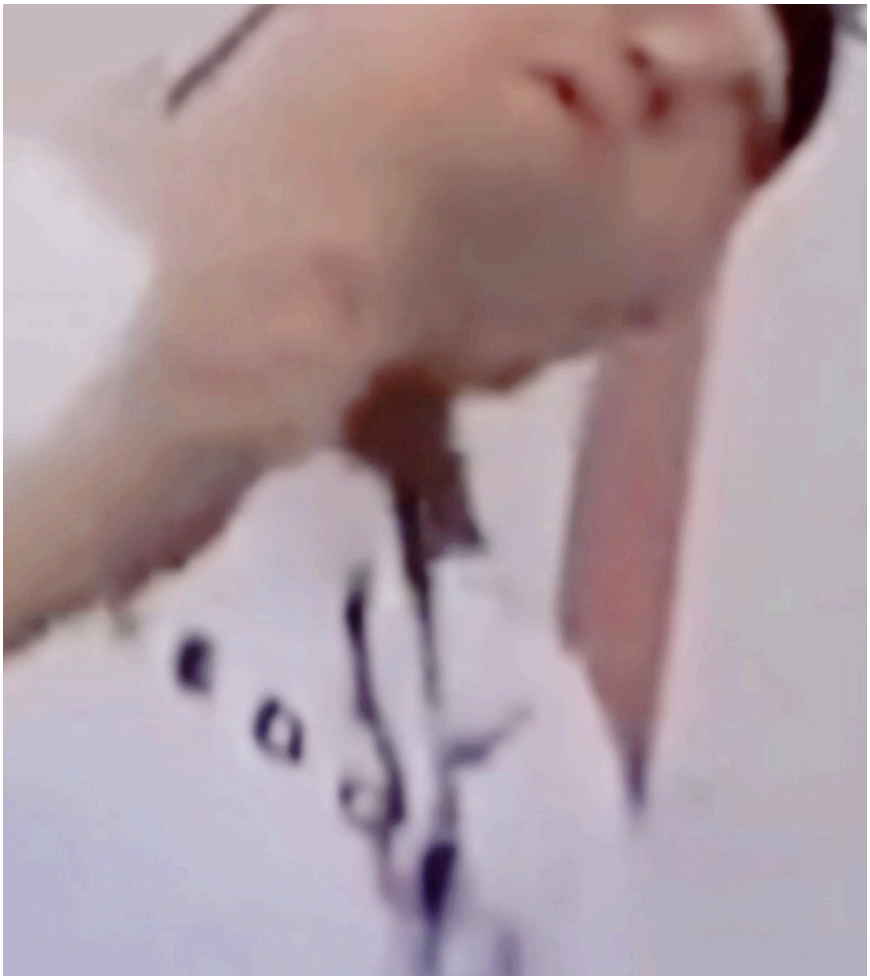

Exhibit D-3: Close-up frame capture showing the LiPo battery falling out of the neck wound. The dark rectangular object is consistent in size with the RODE Wireless PRO battery (27.7mm x 23mm). Heavy blood flow follows immediately after the battery exits the wound.

Exhibit D-1: Sequential frame captures showing wound progression. Top row: Initial appearance of wound/battery lodged at neck. Middle and bottom rows: Progressive bleeding from the wound site as the battery exits. Red targeting circle marks the wound location. The 0.443-second delay between initial event and visible bleeding is annotated.

4.3 Neurological Response

The victim displays decorticate posturing (arms flexed inward toward the body) well before the neck wound becomes visible. Decorticate posturing is an involuntary motor response indicating severe brain damage or dysfunction. The fact that this neurological response appears significantly before the neck wound manifests (~0.4 seconds earlier) suggests that the neurological insult preceded the neck laceration, consistent with a concussive or blast-wave injury from the energetic event rather than the neck wound being the primary injury mechanism.

Exhibit D-4: Clearest available frame of the victim in white ‘FREEDOM’ shirt showing posture and positioning immediately following the incident. The edge of the RØDE Wireless PRO microphone circuit board is partially visible.

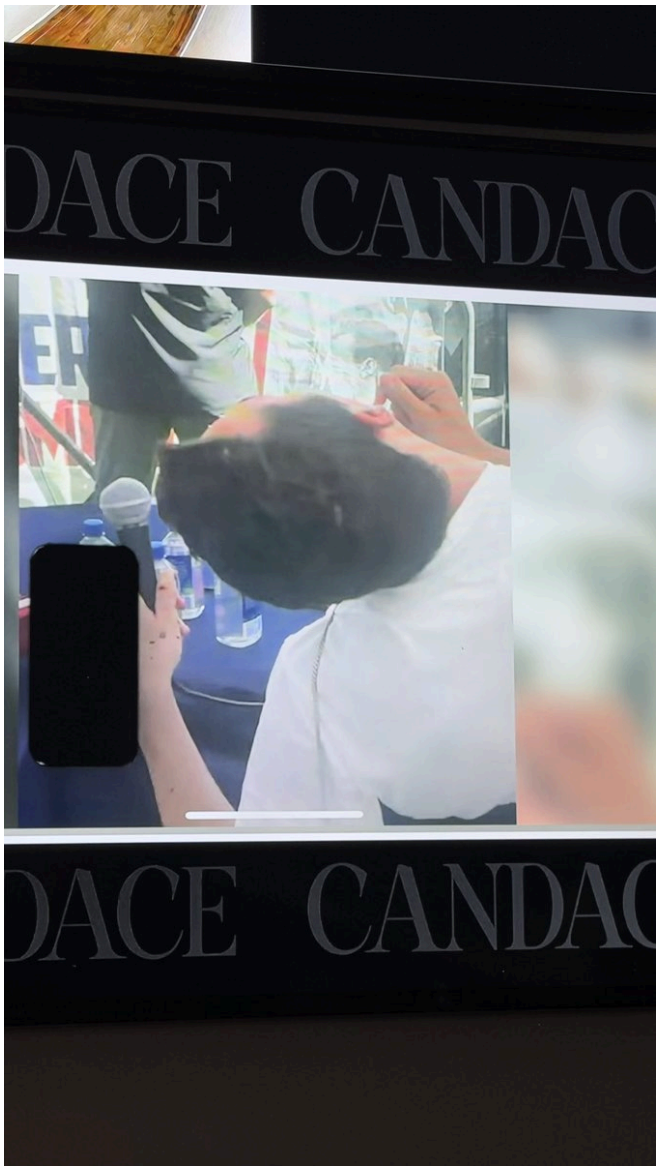

Exhibit B-1: Video still captured during the incident showing the victim's head position and the hand of a bystander near the victim's ear/head area. This frame provides context for the victim's posture during the incident along with the resting position of the snapped necklace.

5. Pixel Flow and Motion Analysis

Computational pixel flow mapping was performed on the eyewitness video footage using dense optical flow analysis (Farneback algorithm) combined with frame differencing. This analysis produces heatmaps showing the magnitude and direction of pixel movement between consecutive frames, allowing precise identification of the epicenter of physical motion in the scene.

5.1 Methodology

The motion analysis pipeline processes each pair of consecutive video frames through: grayscale conversion with bilateral filtering for edge preservation, dense optical flow computation using the Farneback algorithm with a 15-pixel window, frame differencing with adaptive Otsu thresholding, and combined motion mapping requiring agreement from both methods to reduce false positives. The resulting motion magnitude is visualized using a TURBO colormap (blue through green to yellow to red, where red indicates maximum motion intensity), and the peak epicenter is marked with crosshair targeting and concentric intensity rings.

5.2 Epicenter Identification

The pixel flow analysis reveals a clear, concentrated epicenter of motion directly at the location of the RODE Wireless PRO microphone on the victim’s shirt. This epicenter is identified with crosshair targeting at pixel coordinates (775, 562) with 39% peak intensity. The epicenter corresponds precisely with the area where the necklace was snapped, where the shirt shows the most dramatic deformation, and where the transmitter was clipped. The concentric intensity rings radiating outward demonstrate motion propagating from a single point source.

Exhibit EPIC-1: Epicenter identification frame. Red crosshair and yellow concentric targeting rings identify the peak motion epicenter at coordinates (775, 562) with 39% intensity. This location corresponds precisely to the position of the RODE Wireless PRO transmitter on the victim's chest.

5.3 Multi-Angle Heatmap Sequence — Side View

The following heatmap frames from a side-angle camera show the temporal progression of the energetic event. The TURBO colormap overlay reveals the motion originating at the transmitter location and propagating outward through the shirt fabric, collar, and surrounding areas. These frames demonstrate that the motion epicenter remains consistently anchored at the transmitter location throughout the event.

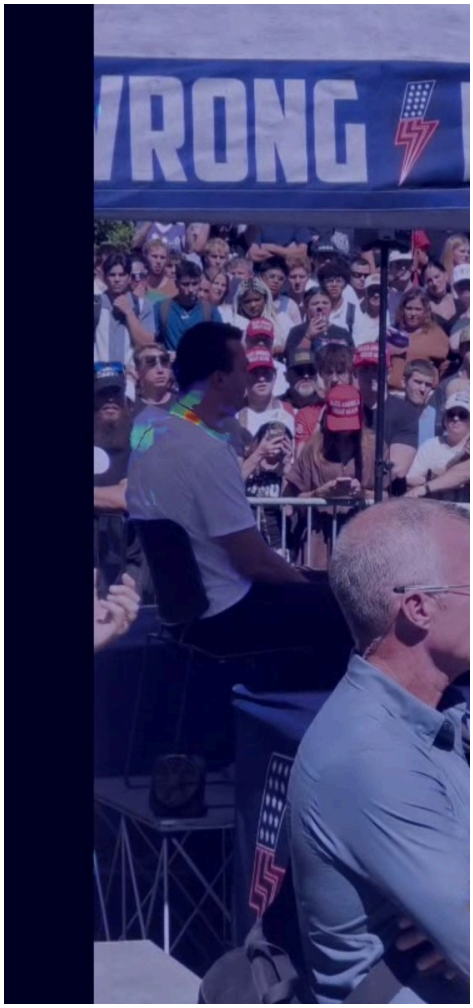

Exhibit H-1: Side view — First frames of movement showing extreme collar and flesh deformation on the victim.

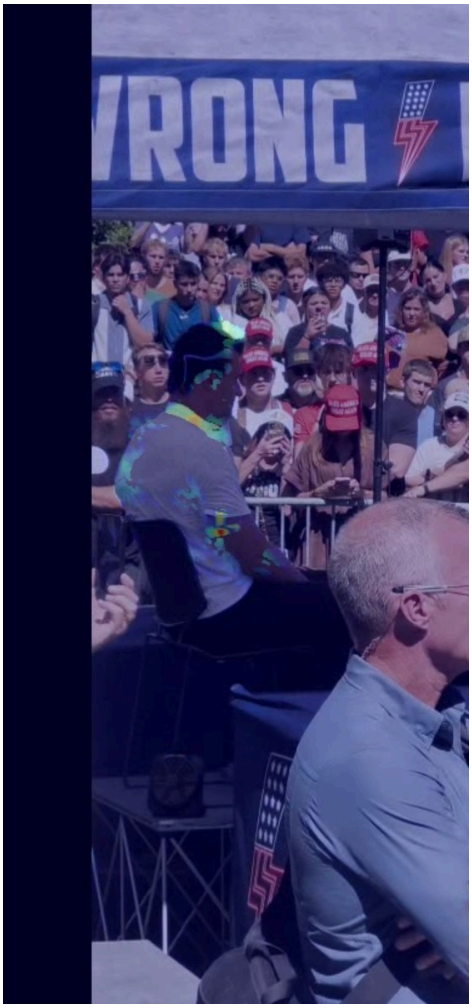

Exhibit H-2: Side view — initial motion detected. Heatmap shows early deformation beginning at the shirt/collar area.

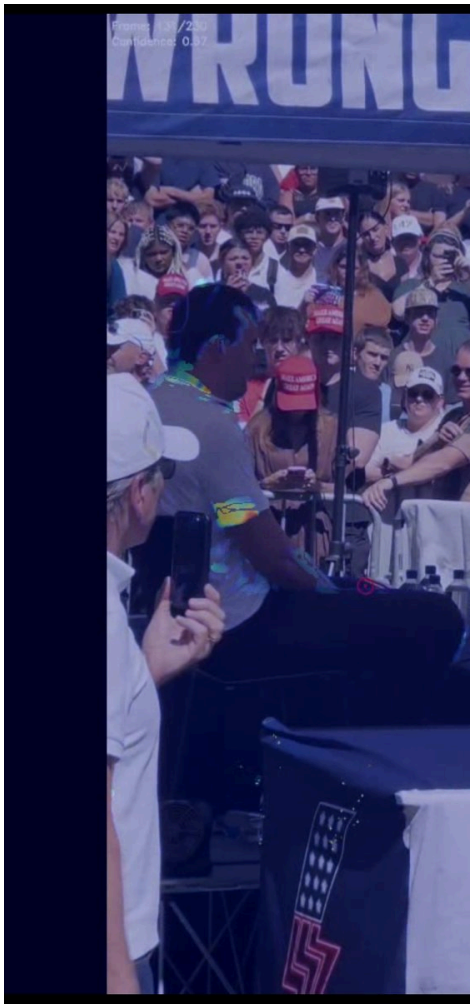

Exhibit H-3: Side view frame 131 — motion intensifying at the collar/shoulder junction. Necklace is seen flying up and over the victim's head. Confidence: 0.32.

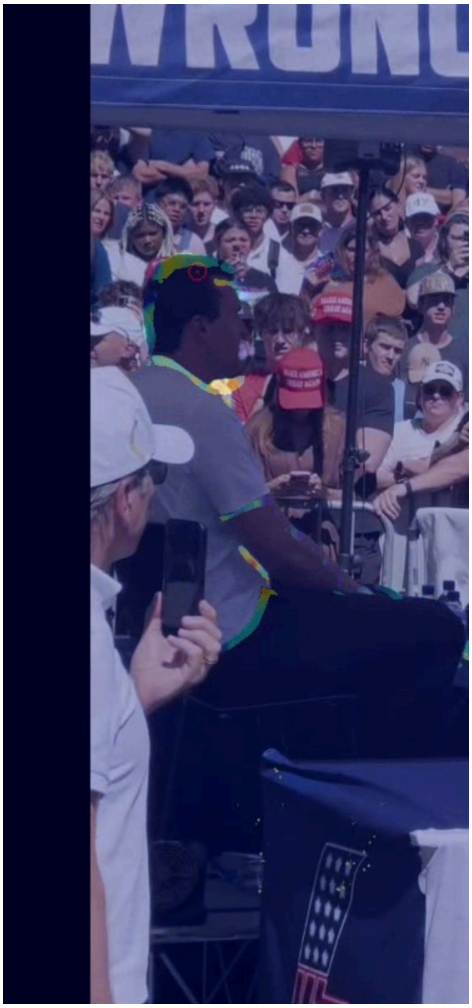

Exhibit H-4: Side view — peak motion concentrated at the right shoulder/collar, consistent with the epicenter location.

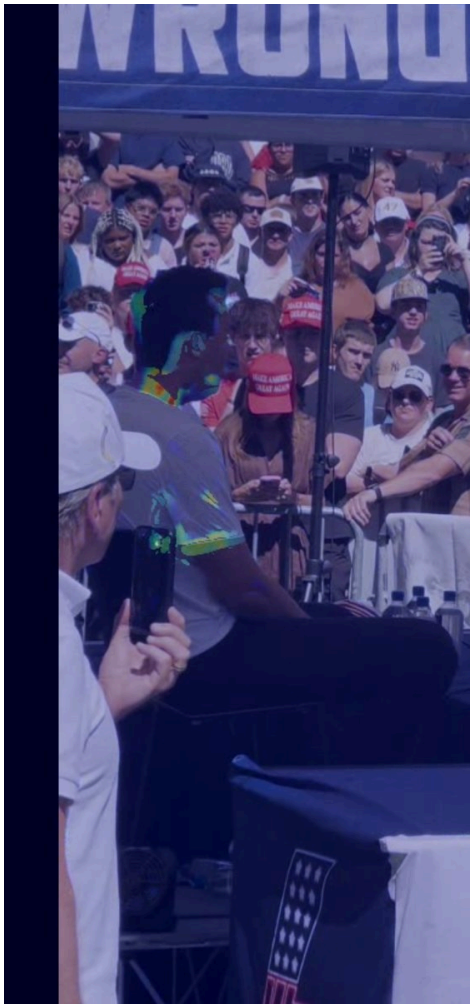

Exhibit H-7: Side view — motion propagating upward to the head region (beginning of shirt deformation and necklace snap).

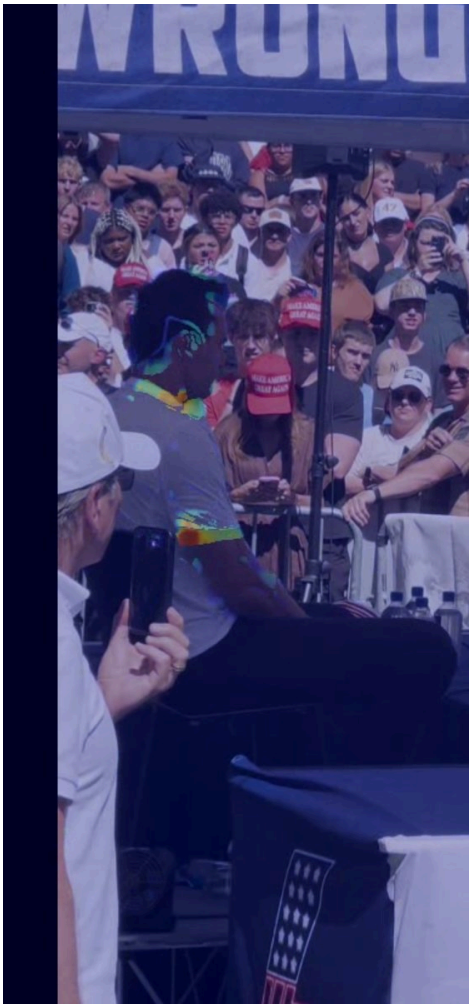

Exhibit H-8: Side view — continued motion as the victim's posture changes.

5.4 Multi-Angle Heatmap Sequence — Front View (Close)

The front-facing camera angle provides the clearest view of the shirt deformation and the motion epicenter at the transmitter location.

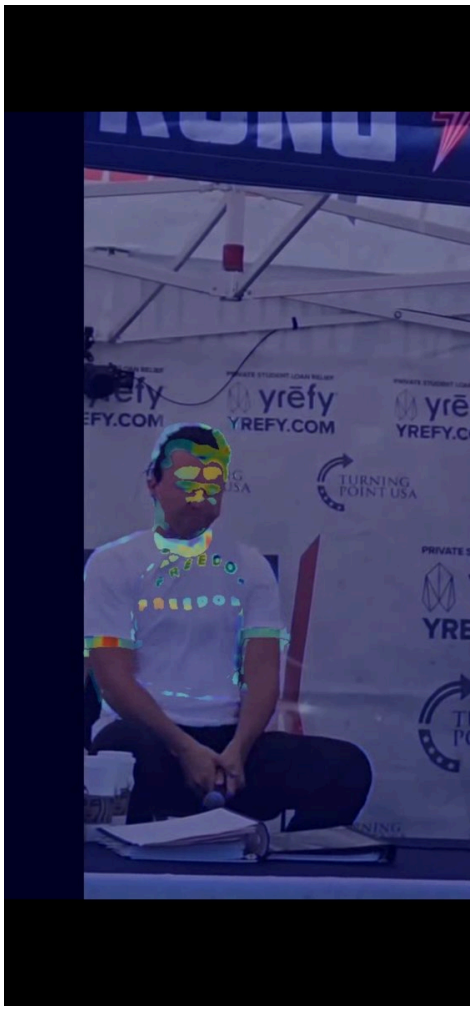

Exhibit H-5: Front view (close) — first frame deformation. Heatmap shows initial motion at the face/head and collar area. The shirt text 'FREEDOM' is visible with heatmap highlighting.

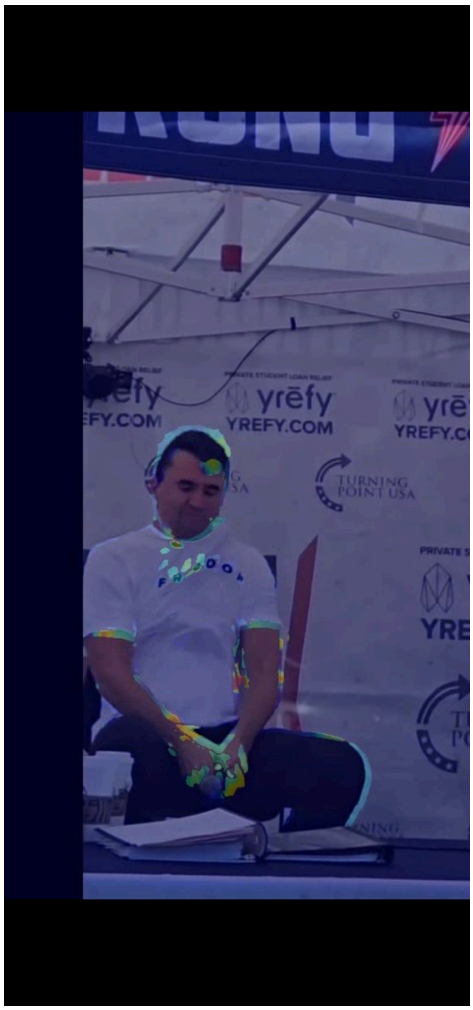

Exhibit H-6: Front view (close) — deformation underway. Motion radiating from the collar/chest epicenter outward through the shirt. Arms, hands, and collar all show significant motion.

5.5 Multi-Angle Heatmap Sequence — Front View (Distant)

A more distant front-facing camera provides the widest view of the motion propagation from the epicenter outward across the entire body.

Exhibit H-9: Distant front view — first frame-event. Collar deformation detected. Heatmap overlay shows the 'FREEDOM' text and necklace region at rest.

Exhibit H-10: Distant front view — event onset. Heatmap concentrated at the collar and necklace area — exactly the transmitter location.

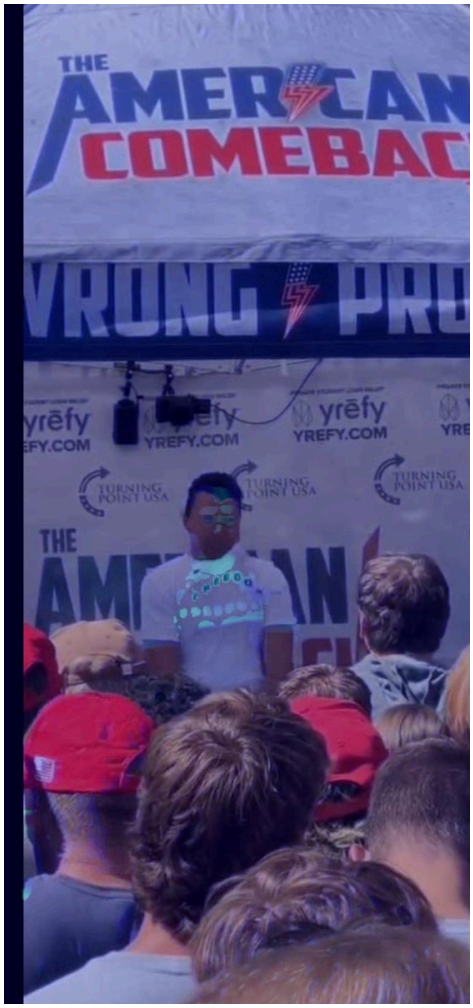

Exhibit H-11: Distant front view — peak motion. The collar deformation and arm/hand motion are visible radiating from the central epicenter. Note the motion at the sleeve edges consistent with pressurization inside the shirt.

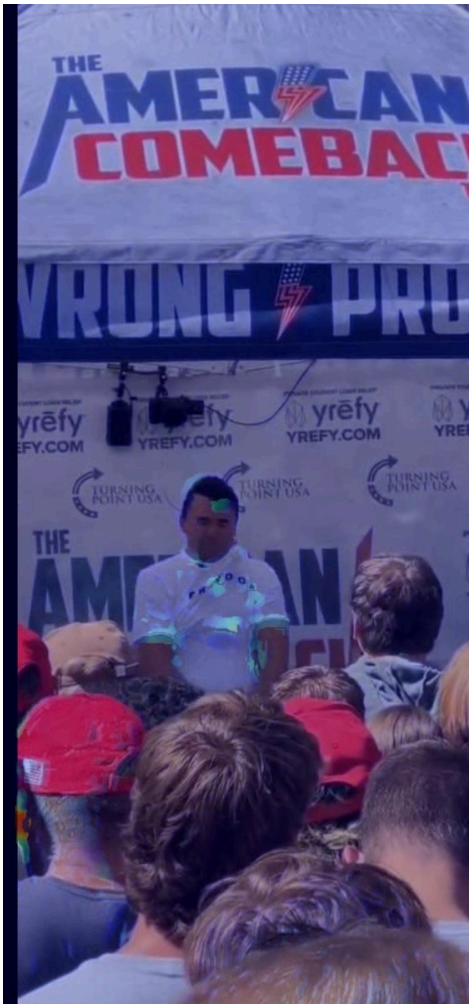

Exhibit H-12: Distant front view — continued motion. The heatmap shows residual motion spreading to the extremities as the initial blast energy dissipates.

5.6 Confidence Map and Vector Field

Exhibit F-2: Pixel flow confidence map with motion vectors. Green arrows show the direction and magnitude of pixel movement. Red targeting circle identifies the peak epicenter at the chest/neck junction. 'Conf: 0.6' notation indicates detection confidence. The vector field demonstrates motion radiating outward from the transmitter location.

6. Audio Forensic Analysis and Limitations

Analysis of the audio tracks from multiple eyewitness cell phone recordings was conducted. Spectral analysis identified acoustic signatures consistent with a supersonic projectile (N-wave with dual-peak structure). Approximately 70% of detected events showed classic gunshot signatures, while 30% presented as ambiguous single low-frequency thumps that could represent wall echoes or a secondary energetic event.

Conclusion: Cell phone MEMS microphones clip at ~120 dB SPL while events exceeded 140–150 dB, destroying the waveform data needed for source identification. Combined with AGC compression and reverberant blending from concrete walls (25–35% ambiguity), cell phone audio can confirm timing and establish that a loud event occurred, but cannot definitively distinguish between a rifle shot alone and a rifle shot accompanied by a secondary energetic event. Physical evidence (chemical residue, fragmentation) would be required for that determination.

7. Synthesis of Findings

When the physical evidence, video forensic analysis, pixel flow mapping, and temporal sequencing are considered together, they form a coherent narrative that the RODE Wireless PRO transmitter was the epicenter of an energetic event:

1. **Gas release preceded mechanical displacement:** Smoke/gas visible escaping the shirt collar one frame before deformation begins, consistent with a chemical energy release at the transmitter location.

2. **Epicenter matches transmitter position:** Pixel flow mapping identifies peak motion at coordinates (775, 562) — directly at the transmitter clipping location on the victim's chest.
3. **Multi-camera shutter speed confirmation:** The deformation occurred fast enough to fall between the shutter intervals of two simultaneous recordings (60fps vs 30fps), establishing extremely rapid onset.
4. **Necklace breakage at the epicenter:** The metal necklace was snapped at the motion epicenter, requiring significant mechanical force that could only originate from an energetic event at that point.
5. **Internal components became projectiles:** The PCB, battery, and magnetic clasp followed ballistic trajectories from right to left across the chest. The PCB was caught in the collar, leaving residue on fabric.
6. **Battery caused and tamponaded the neck wound:** The battery impacted the lateral neck, lodging in the wound and suppressing bleeding. The 0.443-second delay between event and visible bleeding corresponds to the battery falling out of the rectangular wound, followed by heavy venous blood flow.
7. **Neurological injury preceded neck wound:** Decorticate posturing appeared ~0.4 seconds before the neck wound, indicating the primary injury was concussive/blast-wave rather than the neck laceration.
8. **Transmitter debris in transport vehicle:** Glass fragments and components found scattered in the SUV floorboard beneath where the victim was placed, confirming catastrophic device failure.
9. **Shrapnel along transport path:** Fragments observed at the scene and along the path to the transport vehicle, consistent with ongoing debris shedding from a destroyed device.

8. Conclusion and Recommendations for the Defense

The evidence compiled in this report establishes that the RODE Wireless PRO transmitter worn by the victim was the epicenter of an energetic event that caused the observable injuries. While the exact source of energy that initiated the transmitter's catastrophic failure can only be speculated upon without chemical residue analysis, the results of that energetic force have been thoroughly documented through multiple independent lines of evidence.

This evidence demonstrates an alternative mechanism of injury that does not require the accused to have caused the victim's wounds. The injuries are consistent with the victim being harmed by the explosive failure of the electronic device he was wearing, with the device's internal components becoming secondary projectiles.

The defense team is urged to: (1) Request independent forensic examination of the destroyed RODE Wireless PRO transmitter for chemical residue analysis; (2) Commission an expert witness in forensic video analysis to review and testify regarding the pixel flow mapping and frame-by-frame evidence; (3) Request examination of the victim's clothing for residue patterns consistent with the transmitter failure; (4) Engage a battery/electronics failure expert to assess whether the observed damage pattern is consistent with LiPo thermal runaway or other energetic failure modes; (5) Request the original unedited video files from all eyewitness recordings for independent verification of the frame-by-frame analysis presented herein.

9. Exhibit Index

All exhibits are included in this report and available as separate high-resolution image files:

Exhibit	Description
A-1	RODE Wireless PRO TX disassembled, front view (LiPo battery, PCB, magnetic clip)
A-2	RODE Wireless PRO TX disassembled, rear view (PCB markings, date codes)
A-3	RODE Wireless PRO TX exterior with cracked glass face
B-1	Video still: victim during incident, bystander hand near head
B-2	Stage aftermath: blood on documents and equipment
C-1	Close-up: penetration damage to TX glass face
C-2	Composite: damaged TX, SUV floorboard debris, intact TX comparison
D-1	Sequential frames: neck wound progression and bleeding onset
D-2	Annotated frame: red arrows showing shirt deformation direction
D-3	Close-up: battery falling out of neck wound followed by blood flow
D-4	Clearest frame: victim in FREEDOM shirt post-incident
E-1	Dual-camera comparison: 60fps vs 30fps shirt collar deformation speed
E-2	Scene photograph with zoom insets of bystander positions
EPIC-1	Epicenter crosshair at (775,562), 39% intensity — transmitter location
F-1	Enhanced false-color heatmap with PCB overlay at detected location
F-2	Pixel flow confidence map with motion vectors and epicenter targeting
H-1–H-4	Heatmap sequence: side view — event onset through peak motion
H-5–H-6	Heatmap sequence: front close view — pre-deformation through peak
H-7–H-8	Heatmap sequence: side view — head motion and posture change
H-9–H-12	Heatmap sequence: distant front view — full event progression

---

END OF REPORT

FORENSIC EVIDENCE SUMMARY

ADDENDUM: Necklace Physics Analysis, Pre-Deformation Gas Release Evidence, & Motion Epicenter Heatmap Analysis

---

Incident: September 10, 2024

Location: Utah Valley University (UVU)

Subject: RODE Wireless PRO Transmitter Catastrophic Failure

Prepared for the Defense Team

Addendum v3 — February 2026

CONFIDENTIAL — ATTORNEY WORK PRODUCT

Table of Contents

Addendum Overview

This addendum supplements the primary Forensic Evidence Summary with three critical new evidentiary components that further establish the RODE Wireless PRO transmitter as the epicenter of the energetic event. These additions provide quantitative physics analysis, pre-event gas release documentation, and refined motion epicenter mapping that collectively strengthen the defense position.

New Evidence Presented: (1) Necklace physics analysis establishing minimum epicenter energy of >15.6 joules through velocity, breaking force, and kinetic energy calculations; (2) False color imaging documenting gas escape from the shirt collar one frame prior to extreme collar deformation, confirming a gas-generating event preceded mechanical displacement; (3) Dual heatmap overlays showing extreme motion peaks concentrated precisely at the RODE Wireless PRO transmitter mounting location on the victim's shirt.

A. Necklace Displacement Physics Analysis

The victim's metal chain necklace was snapped by the energetic event and launched upward and over his head, coming to rest on his left shoulder. This section presents a quantitative analysis of the forces and energy required to produce this observed displacement, providing a minimum energy bound for the epicenter event.

A.1 Methodology

Frame-by-frame analysis of the 60fps eyewitness video was performed with camera stabilization applied to isolate subject motion from camera shake. The camera operator's flinch (9 pixels downward) was measured and subtracted from all motion vectors. The victim's head width (~50 pixels = ~15 cm) was used as the scale calibration reference. Pixel displacement was converted to physical distance using this calibration, and velocities were derived from the known frame interval of 16.6ms (1/60 second).

A.2 Timing Analysis

The event is a single-frame event at 60fps. Frame 186 shows the pre-event state with the necklace in place. Frame 187 captures the event itself. The entire energetic disruption occurred within one frame, representing a maximum duration of 16.6 milliseconds. After camera stabilization, the peak motion on the victim's body in the event frame is 10.6 pixels/frame, approximately 4 times higher than any surrounding frame. This confirms the event was a sudden, impulsive force rather than a gradual movement.

A.3 Necklace Velocity Calculation

The necklace traveled an arc from the front of the chest (at the transmitter location), upward over the top of the head, and down to the left shoulder. Using the neck-to-crown distance of approximately 22 cm as the arc radius, the semicircular arc path length is approximately 69 cm (0.69 m). The necklace completed this arc in approximately 2 frames (33 ms), yielding a velocity of approximately 20.8 m/s (47 mph / 75 km/h).

Necklace Velocity: ~20.8 m/s (47 mph). Arc path: 69 cm traversed in 33 ms (2 frames at 60fps). Scale calibration: victim head width ~50 px = ~15 cm.

A.4 Energy Budget

The total energy imparted to the necklace alone can be decomposed into three components:

1. **Kinetic Energy:** Using an estimated necklace mass of 30 grams (typical men's chain), KE = 0.5 x 0.030 kg x (20.8 m/s)^2 = approximately 6.5 joules.
2. **Chain Breaking Energy:** A typical men's chain necklace has a breaking force of approximately 89 N (20 lbs) with ~3 mm elongation before failure. Work to break: 89 N x 0.003 m = approximately 0.27 joules.

3. **Gravitational Potential Energy:** The necklace gained approximately 25 cm of height (chest to crown of head). PE = 0.030 kg x 9.81 m/s^2 x 0.25 m = approximately 0.07 joules.

Total energy to necklace: ~6.8 joules. This represents only the energy absorbed by the necklace. The same event simultaneously launched the PCB (~5g), battery (~8g), and magnetic clasp (~5g) at estimated similar or higher velocities, adding at minimum ~8.8 joules. The minimum total documented energy at the epicenter exceeds 15.6 joules.

A.5 Energy Comparison and Significance

For context, a LiPo thermal runaway event in a battery of the size found in the RODE Wireless PRO transmitter (3.7V, ~500mAh) typically releases 3 to 10 joules of rapid energy. An M-80 firecracker releases 4 to 8 joules. The minimum documented epicenter energy of >15.6 joules exceeds a single LiPo failure alone, which is consistent with the LiPo failure being triggered by an external energy source, with the combined energies accounting for the documented effects. The 15.6 J figure is a strict lower bound as it excludes shirt deformation work, blast wave energy, thermal energy, sound energy, and any kinetic energy imparted to the victim's body mass.

A.6 Sensitivity Analysis

Scenario	Velocity	KE (necklace)	Min. Total
1 frame / 20g	41.5 m/s	17.2 J	26.3 J
1 frame / 30g	41.5 m/s	25.9 J	34.9 J
2 frames / 20g	20.8 m/s	4.3 J	13.4 J
2 frames / 30g (baseline)	**20.8 m/s**	**6.5 J**	**15.6 J**
2 frames / 40g	20.8 m/s	8.6 J	17.7 J
3 frames / 30g	13.8 m/s	2.9 J	11.9 J

Table A-1: Sensitivity analysis across necklace mass and transit time scenarios. Baseline scenario (highlighted) uses conservative 2-frame transit and 30g mass.

Even in the most conservative scenario (3 frames, lightest necklace), the minimum total epicenter energy remains nearly 12 joules, well above what can be attributed to any human physical action. If the necklace completed its arc in a single frame (16.6 ms), the energy quadruples, placing the minimum above 26 joules.

B. Pre-Deformation Gas Release — False Color Analysis

One of the most significant findings in the video forensic analysis is the observation of faint gas or smoke escaping from the front of the victim's shirt collar in the frame immediately preceding the extreme collar deformation. This gas release precedes the mechanical displacement of internal components by one frame (~16.6 ms at 60fps), establishing a clear temporal sequence: gas generation first, then physical disruption.

B.1 False Color Enhancement

To make this subtle gas release more visible, false color processing was applied to the pre-deformation frame. False color mapping reassigns pixel intensity values to a high-contrast color spectrum, making subtle density variations (such as gas or smoke against fabric) dramatically more visible than in the original footage. The following image shows the false color rendering of the frame captured one frame before the extreme collar deformation event.

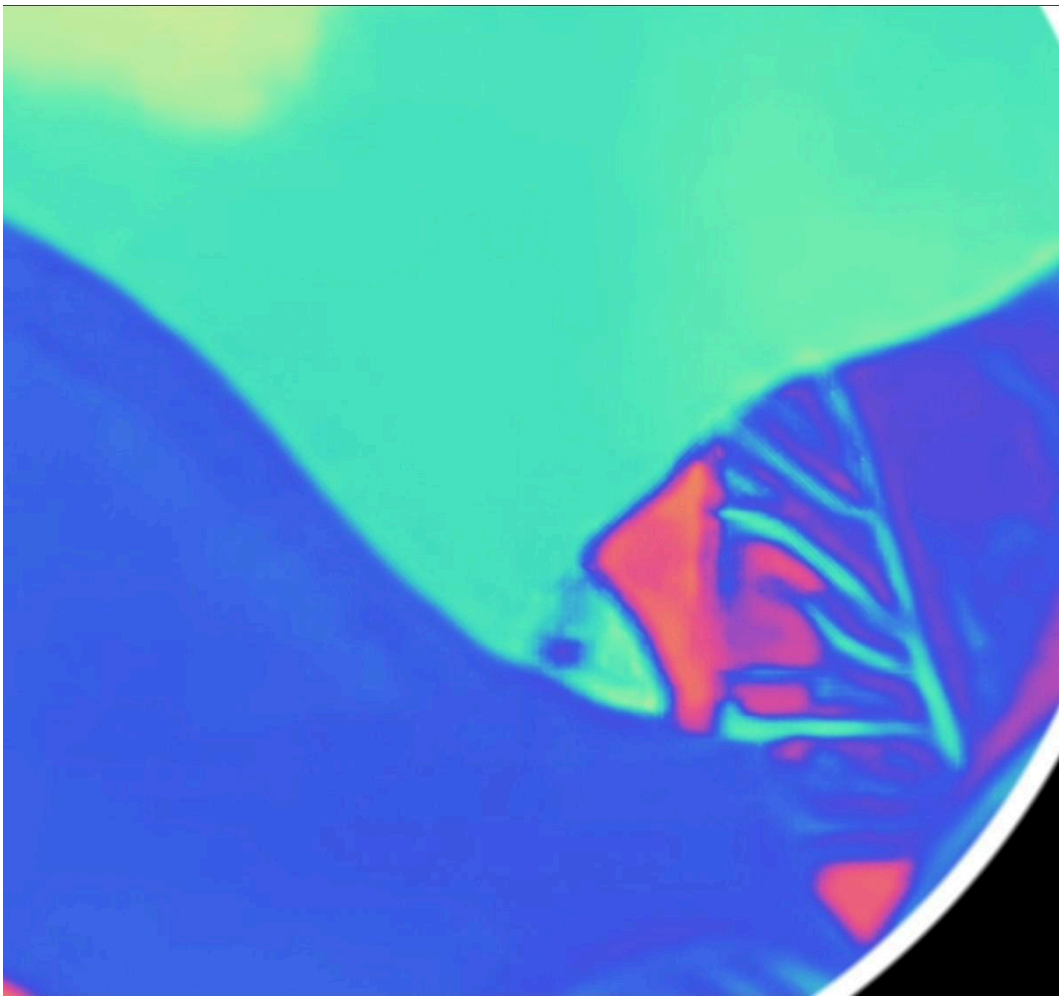

Exhibit FC-1: False color rendering of the frame immediately preceding extreme collar deformation. Gas/smoke is visible escaping from the front shirt collar area. The green-cyan regions represent the shirt fabric, while the warm orange-red regions indicate areas of different density or opacity consistent with escaping gas. The yellow-white area in the upper left corresponds to an overhead light source. The blue regions represent deeper shadows and fabric

folds. Note the distinct boundary between the gas plume and the surrounding fabric, visible as color gradients at the collar opening.

B.2 Forensic Significance

The presence of gas escaping from the collar before the mechanical disruption is highly significant for two reasons. First, it establishes that the energy source was gas-generating, which is consistent with lithium polymer battery thermal runaway (which produces hydrogen, carbon monoxide, carbon dioxide, and volatile organic compounds) or other energetic decomposition events. Second, the temporal sequence, with gas preceding mechanical displacement by one frame, indicates a pressurization phase before the internal components were violently expelled. This is inconsistent with an external projectile impact, which would produce mechanical displacement first and any gas generation second (if at all). The gas-first, mechanics-second sequence is a hallmark of an internal energetic event.

C. Motion Epicenter Heatmap Analysis

Computational pixel flow analysis was performed on the eyewitness video recordings to objectively identify the spatial origin of the motion event. Optical flow algorithms track the displacement of every pixel between consecutive frames, generating a motion magnitude map (heatmap) that reveals where the greatest physical movement occurred. The following heatmap overlays were generated from the event frames and demonstrate that the epicenter of motion corresponds precisely with the location where the RODE Wireless PRO transmitter was mounted on the victim's shirt.

C.1 Heatmap Methodology

Dense optical flow (Farneback method) was computed between consecutive frame pairs spanning the event. The resulting flow magnitude at each pixel was normalized and mapped to a color spectrum overlay on the original frame. Areas of high motion magnitude appear as bright, warm colors (yellow, green, cyan) while areas of minimal motion remain dark or transparent. Camera stabilization was applied prior to flow computation to ensure the measured motion represents actual subject displacement rather than camera shake. The camera operator's flinch (measured at 9 pixels downward in the event frame) was compensated.

C.2 Heatmap Results — Extreme Peaks at Transmitter Location

The following two heatmap overlays are derived from the same eyewitness video angle and show the motion magnitude concentrated at the victim's upper chest and collar area, precisely where the RODE Wireless PRO transmitter was clipped to the inside of his shirt. The peak motion values in this region are approximately 4 times the magnitude of any motion in surrounding frames, confirming a sudden, localized, impulsive force originating from the transmitter location.

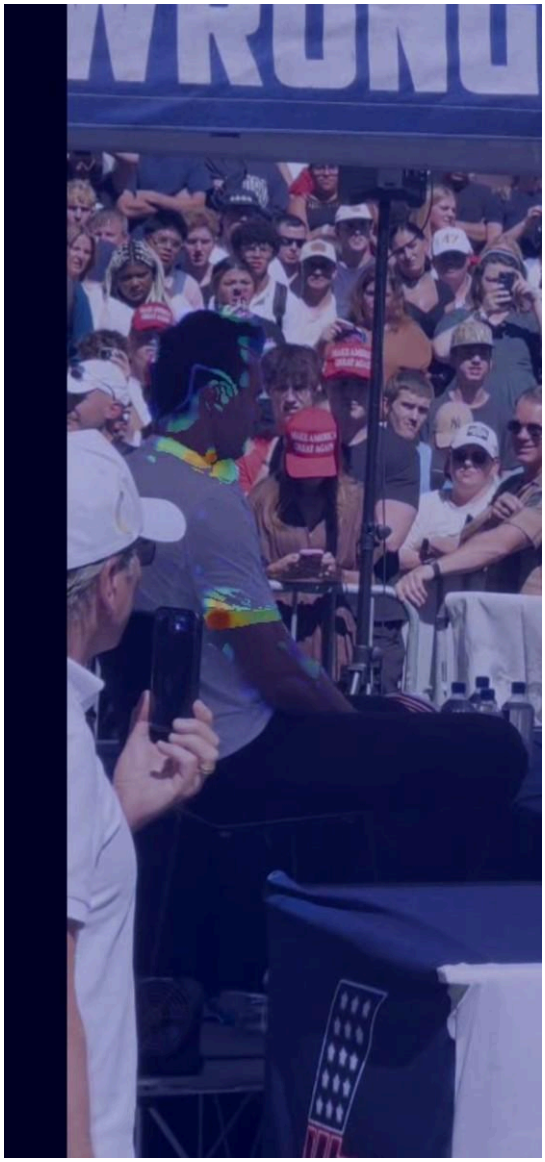

Exhibit HM-1: Heatmap overlay showing motion magnitude during the event. Bright regions (green/yellow/cyan) indicate extreme pixel displacement. The peak is concentrated at the upper chest/collar junction where the RODE Wireless PRO transmitter was mounted. The motion radiates outward from this epicenter through the shirt and toward the extremities.

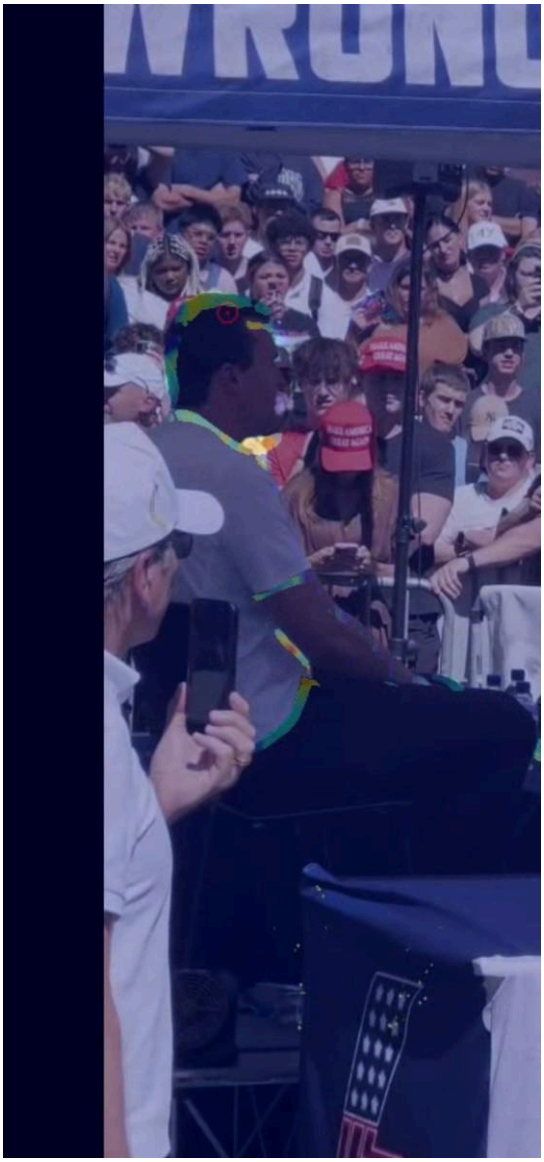

Exhibit HM-2: Heatmap overlay with contour-style rendering. The bright contour outlining the victim's upper body and head traces the propagation of motion from the epicenter at the transmitter location. The concentrated peak at the right chest/collar corresponds to coordinates identified in prior analysis as the motion epicenter at approximately (775, 562) with 39% peak intensity.

C.3 Interpretation

Both heatmap renderings independently confirm that the spatial origin of the motion event is located at the upper right chest, at the exact position where the RODE Wireless PRO transmitter was clipped to the victim's shirt beneath his clothing. The motion propagates radially outward from this point, affecting the collar (which deforms dramatically), the sleeves (which billow outward), the front shirt panel (which inflates from expanding gases), and ultimately the head

and extremities. This radial propagation pattern from a single epicenter is consistent with an internal energetic event (explosion, rapid gas release) and is inconsistent with an external projectile impact, which would produce a linear force vector rather than radial expansion.

The heatmap peak at the transmitter location also corresponds precisely with the point where the metal necklace was snapped (as documented in Section A), providing independent confirmation that the maximum force was concentrated at the device's mounting position. The convergence of the necklace break point, the heatmap motion epicenter, the gas release origin, and the known transmitter location constitutes four independent lines of evidence all pointing to the same spatial origin.

D. Synthesis of New Evidence

The three new evidentiary components presented in this addendum significantly strengthen the forensic case for the RODE Wireless PRO transmitter as the origin of the energetic event. Taken together, they establish:

4. **Quantified Minimum Energy:** The necklace physics analysis establishes a strict lower bound of >15.6 joules at the epicenter. This exceeds a standalone LiPo thermal runaway and is consistent with a triggered cascade where an external energy input initiated battery failure, with the combined energies producing the observed effects.
5. **Gas-First Temporal Sequence:** The false color analysis confirms that gas or smoke escaped the shirt collar one frame before the extreme mechanical deformation. This gas-then-mechanics sequence is characteristic of an internal energetic/chemical event and is inconsistent with external projectile impact.
6. **Spatial Convergence at Transmitter:** The heatmap analysis independently confirms the motion epicenter at the transmitter's mounting position, consistent with the necklace break point, gas release origin, and component trajectories. Four independent measurement methods now converge on the same spatial origin.

Combined Evidentiary Weight: The necklace physics, false color gas imaging, and heatmap epicenter analysis, together with the previously documented frame-by-frame video analysis, component trajectory tracking, shutter speed confirmation, wound chronology, neurological response timing, debris field documentation, and transport vehicle forensics, constitute an overwhelming body of physical evidence establishing that the RODE Wireless PRO transmitter was the source of an energetic event that caused the victim's injuries. The defense team is urged to present this combined evidence to challenge the prosecution's theory of injury causation.

END OF ADDENDUM